

ABC: Efficient Selection of Machine Learning Configuration on Large Dataset

Silu Huang^{1*} Chi Wang² Bolin Ding^{3†} Surajit Chaudhuri²

¹University of Illinois, Urbana-Champaign, IL

²Microsoft Research, Redmond, WA

³Alibaba Group, Bellevue, WA

shuang86@illinois.edu, {wang.chi, surajitc}@microsoft.com, bolin.ding@alibaba-inc.com

Abstract

A machine learning configuration refers to a combination of preprocessor, learner, and hyperparameters. Given a set of configurations and a large dataset randomly split into training and testing set, we study how to efficiently select the best configuration with approximately the highest testing accuracy when trained from the training set. To guarantee small accuracy loss, we develop a solution using confidence interval (CI)-based progressive sampling and pruning strategy. Compared to using full data to find the exact best configuration, our solution achieves more than two orders of magnitude speedup, while the returned top configuration has identical or close test accuracy.

Introduction

Increasing the productivity of data scientists has been a target for many machine learning service providers, such as Azure ML, DataRobot, Google Cloud ML, and AWS ML. For a new predictive task, a data scientist usually spends a vast amount of time to train a good ML solution. A proper *configuration*, i.e., the combination of preprocessor (e.g., feature engineering), learner (i.e., training algorithm) and the associated hyperparameters, is critical to achieving good performance. It often takes tens or hundreds of trials to select a suitable configuration.

There are AutoML tools like auto-sklearn (Feurer et al. 2015) to automate these trials, and output a configuration with highest evaluated performance. However, both the manual and AutoML approaches have become increasingly inefficient as the available ML data volume grows to millions or more. Even the trial for a single configuration can take hours or days for such large-scale datasets. Motivated by this efficiency issue, we propose a module called *approximate best configuration* (ABC). Given a set of configurations, it outputs the approximate best configuration, such that the accuracy loss to the best configuration is below a threshold. Our goal is to *efficiently* select the approximate best configuration.

The intuition behind ABC is that the ML model trained over a sampled dataset can be used to approximate the model trained over the full dataset. However, the optimal sample size to determine the best configuration up to an accuracy

loss threshold is unknown. We develop a novel confidence interval (CI)-based progressive sampling and pruning solution, by addressing two questions: (a) *CI estimator*: given a sampled training dataset, how to estimate the confidence interval of a configuration’s real performance with full training data? (b) *scheduler*: as the optimal sample size is unknown *a priori*, how to allocate appropriate sample size for each configuration?

Our contributions are summarized as the following.

- We develop an ABC framework using progressive sampling and CI-based pruning. It ensures finding an approximate best configuration while reducing the running time.
- We present and prove bounds for the real test accuracy when the ML model is trained using full data, based on the model trained with sampled data.
- Within ABC, we design an approximately optimal scheduling scheme based on the confidence interval, for allocating sample size among different configurations.
- We conduct experiments with large datasets. We demonstrate that our ABC solution is tens to hundreds of times faster, while returning top configurations with no more than 1% accuracy loss.

Problem Formulation

Notions and Notations. In this paper, we focus on classification tasks with a large set of labeled data \mathcal{D} . In order for reliable evaluation of a trained classifier, data scientists usually split the available data *randomly* into training and testing set \mathcal{D}_{tr} and \mathcal{D}_{te} . After that, they specify a number of configurations of the ML workflow and try to select the best configuration. Let \mathcal{C} be the candidate configuration set and C_i be the i^{th} configuration in \mathcal{C} . We further let n be the number of configurations, i.e., $n = |\mathcal{C}|$. Using terminology from learning theory, each configuration C_i defines a *hypothesis space* \mathcal{H}_i , where each *hypothesis* $H \in \mathcal{H}_i$ is a possible classifier trained under this configuration. Given a training dataset \mathcal{D}_{tr} , the learner in C_i will output a hypothesis $H_{tr}^i \in \mathcal{H}_i$ as the trained classifier. The quality of the classifier is measured against the heldout testing data \mathcal{D}_{te} . In this paper, we focus on *accuracy* as the quality metric. We denote the accuracy of hypothesis $H \in \mathcal{H}_i$ on dataset D as $\mathcal{A}(H, D)$. In particular, given a configuration C_i , we define its *real test accuracy* as $\mathcal{A}_i = \mathcal{A}(H_{tr}^i, \mathcal{D}_{te})$.

*Work done while visiting Microsoft Research

†Work done while working in Microsoft Research

\mathcal{C}	configuration set	C_i	one configuration in \mathcal{C}
\mathcal{H}_i	hypothesis class of C_i	H_{tr}^i	hypothesis trained with \mathcal{D}_{tr} under C_i
\mathcal{A}_i	real test accuracy for $C_i \in \mathcal{C}$	\mathcal{D}_{te}	test dataset
\mathcal{D}	full dataset	\mathcal{D}_{tr}	training dataset
S_{tr}	sample set from \mathcal{D}_{tr}	S_{te}	sample set from \mathcal{D}_{te}
t_i	total running time for C_i	l_i	lower bound of \mathcal{A}_i
u_i	upper bound of \mathcal{A}_i	n	$n = \mathcal{C} $

Table 1: Notations

Problem Definition. A standard practice to select the best configuration from a configuration set \mathcal{C} is to train with each configuration using full training data, and then pick the one with the highest test accuracy, i.e., $i^* = \arg \max_{i \in [n]} \mathcal{A}_i$. Note that an implicit assumption made here is that the returned classifier with full training data has equal or higher test accuracy than the classifier trained with sampled training data. We call this *exploitiveness* assumption and follow it in this paper. From a user’s perspective, if there are multiple configurations with nearly identical highest real test accuracy, then it would suffice to return any of them as the best configuration. So we introduce a new problem *approximate best configuration selection*, as formalized in Problem 1.

Problem 1 (Approximate Best Configuration Selection). *Given a configuration candidate set \mathcal{C} and an accuracy loss tolerance ϵ , select a configuration $C_{i'}$ whose real test accuracy is within ϵ away from that of the best configuration C_{i^*} , i.e., $\mathcal{A}_{i^*} - \mathcal{A}_{i'} \leq \epsilon$, and minimize the total running time.*

CI-based Framework

Before introducing our framework, we first describe some insights based on simple observations. We experiment on the *FlightDelay* dataset with five learners (as five configurations). Readers can refer to Table 2 for detailed statistics of this dataset. The *learning curve* for each configuration is depicted in Figure 1, where x-axis is the training sample size in log-scale and y-axis is the test accuracy on \mathcal{D}_{te} . In general, the test accuracy approaches the real test accuracy with the increase of the training sample size. When the sample size is large enough ($\geq 2M$), the configuration with the highest test accuracy is LightGBM – the true best configuration. If we knew it before the experiment, we could use a fraction of the training data to select the right configuration.

Furthermore, the optimal sample size to minimize the running time could vary for different configurations. If we magically knew that we should use 2M training samples for LightGBM and 16K training samples for all the other configurations, we could save more time and still identify the correct best configuration. Unfortunately, the optimal sample size for each configuration is unknown. A natural idea is to increase the sample size gradually, until a plateau is reached in the learning curve. However, a naive plateau estimator based on the learning curve is error-prone. As shown from Figure 1, LightGBM’s learning curve is flat from 32K to 128K. If we stopped increasing the sample size for it, it would be mis-pruned. Therefore, a more robust strategy is needed.

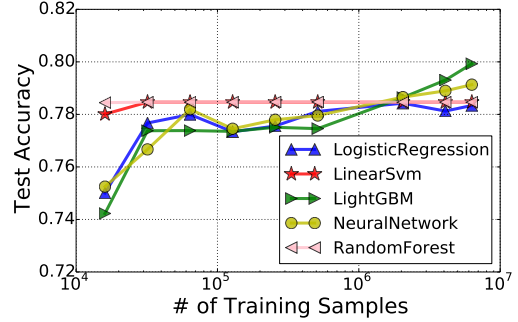


Figure 1: Learning Curve

Overview. The main idea is to estimate the *confidence interval* (CI) of each configuration’s real test accuracy with sampled data, instead of simply using a point estimation of the real test accuracy. In each round, we train the classifier for a selected configuration on some sampled training data. We call such a round of training a *probe*. After a probe, we update the confidence interval for the configuration. As the sample size increases, the confidence interval shrinks, and the badly-performing configurations can be pruned based on the CIs. The pruning based on CI is more robust than based on random observations from the learning curve.

Algorithm 1: ABC

```

1 Input: configuration set  $\mathcal{C}$ , accuracy loss threshold  $\epsilon$ ;
2 Output: the approximate best configuration;
3 Initialization:  $C_{prob} \leftarrow C_1, C_{i'} \leftarrow C_1, \Omega \leftarrow \mathcal{C}$ ;
4 while  $|\Omega| > 1$  do
5   PROBE( $C_{prob}$ );
6    $[C_{prob.l}, C_{prob.u}] \leftarrow$  CIESTIMATOR( $C_{prob}$ );
7   if  $C_{prob.l} > C_{i'.l}$  then  $C_{i'} \leftarrow C_{prob}$ ;
8   for  $C \in \Omega$  do // pruning
9     if  $C.u - C_{i'.l} \leq \epsilon$  then  $\Omega \leftarrow \Omega - C$ ;
10  if Pruning happens then
11    for  $C \in \Omega$  do
12       $C.u_{old} \leftarrow C.u; C.l_{old} \leftarrow C.l$ ;
13     $C_{prob} \leftarrow$  SCHEDULER( $\Omega$ )
14 return  $C_{i'}$ ;

```

Detailed Algorithm. ABC proceeds round by round as shown in Algorithm 1, where each configuration C_i is annotated with its current sample size ($C_i.s$), current lower bound

Name	$ \mathcal{D} $	$ \mathcal{F} $	Origin
Twitter	1.4M	9866	http://www.sentiment140.com
FlightDelay	7.3M	630	https://catalog.data.gov/dataset/airline-on-time-performance-and-causes-of-flight-delays-on-time-data
NYCTaxi	10M	21	http://www.nyc.gov/html/tlc/html/about/trip_record_data.shtml
HEPMASS	10M	28	https://archive.ics.uci.edu/ml/datasets/HEPMASS
HIGGS	10.6M	28	https://archive.ics.uci.edu/ml/datasets/Higgs

Table 2: Dataset Description. $|\mathcal{D}|$ and $|\mathcal{F}|$ are the number of records and features respectively

($C_i.l$), current upper bound ($C_i.u$), and the cached lower bound ($C_i.l_{old}$) and upper bound ($C_i.u_{old}$) in the recent pruning round. In each round within the while loop (line 4), it first probes the configuration C_{prob} (line 5). Then it calls a CIESTIMATOR subroutine to quickly estimate the confidence interval for \mathcal{A}_{prob} (line 6). Next, it prunes badly-performing configurations (line 7-9). Line 7 identifies the configuration C_i with the largest lower bound. Line 8-9 prunes a configuration if its upper bound is within ϵ away from the largest lower bound. If any configuration is pruned (line 10), we call this iteration a *snapshot* and will update $C.l_{old}$ and $C.u_{old}$ for each configuration C in this snapshot (line 11-12). At last, it calls a SCHEDULER subroutine to determine which configuration to probe next as well as its sample size (line 10).

We describe CIESTIMATOR and SCHEDULER in the next two sections.

CI Estimator

In this section, we will derive a CIESTIMATOR for each configuration’s real test accuracy, based on the probe over sampled data. For configuration C_i , the confidence interval $[l_i, u_i]$ needs to contain the real test accuracy \mathcal{A}_i with high probability. The computation of l_i and u_i needs to be efficient, i.e., no slower than the probe. In the following, we assume i is fixed and omit it in the notations.

At the first glance, the CI estimation may remind readers of the generalization error bounds (e.g., VC-bound). The generalization error bound is a universal bound of the difference between each hypothesis’s accuracy in training data and its accuracy in infinite data following the same distribution. Nevertheless, the confidence interval we need is the range of the real test accuracy of the hypothesis H_{tr} trained from full training data, while we only have the hypothesis $H_{S_{tr}}$ trained from a sample $S_{tr} \subset D_{tr}$. Therefore, we cannot apply generalization error bound to obtain our confidence interval.

We use Figure 2 to summarize the notations and their relationships which are important for understanding the theoretical results. H_{tr} , $H_{S_{tr}}$, and H^* correspond to the returned hypothesis after training a fixed configuration with full training dataset \mathcal{D}_{tr} , the sampled training dataset S_{tr} , and the full dataset \mathcal{D} respectively. For instance, Figure 2(a) shows the overall derivation relationships among \mathcal{D} , \mathcal{D}_{tr} , \mathcal{D}_{te} , S_{tr} , S_{te} , and $H_{S_{tr}}$. First, the full training data \mathcal{D}_{tr} and the full testing data \mathcal{D}_{te} are randomly split from the whole data \mathcal{D} . Second, the sampled training data S_{tr} and the sampled testing data S_{te} are randomly drawn from the full training data \mathcal{D}_{tr} and full testing data \mathcal{D}_{te} . Last, $H_{S_{tr}}$ is trained from the sampled

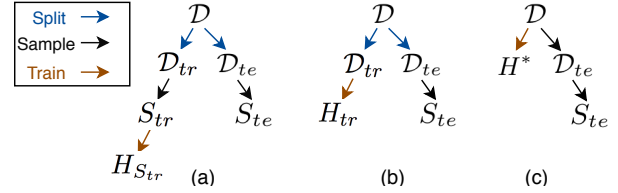


Figure 2: Notations Used in CI Estimation and Analysis

training data S_{tr} . Note that the CI estimator only has access to $H_{S_{tr}}$, S_{tr} and S_{te} . Though H_{tr} and H^* are not accessible, they are useful in our analysis.

Upper bound. The intuition behind the confidence interval estimation is that we need to relate the two hypotheses $H_{S_{tr}}$ and H_{tr} , and use the information we have on $H_{S_{tr}}$ to infer the performance of H_{tr} . To upper bound the accuracy of H_{tr} , we leverage a *fitness* condition: The training process produces a hypothesis that fits the training data. When the configuration is fixed, the accuracy in a dataset D of the hypothesis trained on D should be no lower than the hypothesis trained on a different dataset $D' \neq D$. It is the only assumption we need to prove the upper bound, no matter what training algorithm is used. Under this condition, we found an inequality chain to connect the training accuracy $\mathcal{A}(H_{S_{tr}}, S_{tr})$ to the real test accuracy of H_{tr} .

Theorem 1 (Upper Bound). *Under the fitness condition, with probability at least $1 - \frac{\delta}{2n^2}$, $\mathcal{A}(H_{tr}, \mathcal{D}_{te}) \leq u$, where*

$$u \triangleq \mathcal{A}(H_{S_{tr}}, S_{tr}) + \left(\frac{1}{2|S_{tr}|} \ln \frac{4n^2}{\delta}\right)^{\frac{1}{2}} + \left(\frac{1}{2|\mathcal{D}_{te}|} \ln \frac{4n^2}{\delta}\right)^{\frac{1}{2}}$$

Proof. Let us first recall the fitness condition. Given a fixed configuration C_i , let H and H' be the hypothesis returned by training on two different sample sets D and D' , respectively. Note that H and H' are both from the same fixed hypothesis space \mathcal{H}_i . Our assumption is that H has no lower accuracy on D than H' . Symmetrically, H' has no lower accuracy on D' than H .

First, let us break down $\mathcal{A}(H_{tr}, \mathcal{D}_{te}) - \mathcal{A}(H_{S_{tr}}, S_{tr})$ into four clauses, as shown in Equation (1).

$$\begin{aligned} & \mathcal{A}(H_{tr}, \mathcal{D}_{te}) - \mathcal{A}(H_{S_{tr}}, S_{tr}) \\ = & [\mathcal{A}(H_{tr}, \mathcal{D}_{te}) - \mathcal{A}(H^*, \mathcal{D}_{te})] + [\mathcal{A}(H^*, \mathcal{D}_{te}) - \mathcal{A}(H^*, \mathcal{D})] \\ & + [\mathcal{A}(H^*, \mathcal{D}) - \mathcal{A}(H^*, S_{tr})] + [\mathcal{A}(H^*, S_{tr}) - \mathcal{A}(H_{S_{tr}}, S_{tr})] \end{aligned} \quad (1)$$

Since \mathcal{D}_{tr} and \mathcal{D}_{te} are randomly split from \mathcal{D} , we have $\mathcal{D} = \mathcal{D}_{tr} \cup \mathcal{D}_{te}$. Let $x = \frac{|\mathcal{D}_{te}|}{|\mathcal{D}|}$ be the hold-out ratio. For any

$H \in \mathcal{H}$, we have:

$$\begin{aligned} x\mathcal{A}(H, \mathcal{D}_{te}) + (1-x)\mathcal{A}(H, \mathcal{D}_{tr}) &= \mathcal{A}(H, \mathcal{D}) \\ \Rightarrow \mathcal{A}(H, \mathcal{D}_{te}) &= \frac{1}{x}[\mathcal{A}(H, \mathcal{D}) - (1-x)\mathcal{A}(H, \mathcal{D}_{tr})] \end{aligned} \quad (2)$$

Next, apply Equation (2) to the first clause in Equation (1):

$$\begin{aligned} &\mathcal{A}(H_{tr}, \mathcal{D}_{te}) - \mathcal{A}(H^*, \mathcal{D}_{te}) \\ &= \frac{1}{x}[\mathcal{A}(H_{tr}, \mathcal{D}) - \mathcal{A}(H^*, \mathcal{D})] \\ &\quad - \frac{1-x}{x}[\mathcal{A}(H_{tr}, \mathcal{D}_{tr}) - \mathcal{A}(H^*, \mathcal{D}_{tr})] \leq 0 \end{aligned} \quad (3)$$

The inequality is derived from the fitness assumption (recall from Figure 2 that H_{tr} is trained from \mathcal{D}_{tr} and H^* is trained from \mathcal{D}).

Next, we bound the second clause in Equation (1) with Hoeffding inequality: With probability at least $(1 - \frac{\delta}{4n^2})$,

$$\mathcal{A}(H^*, \mathcal{D}_{te}) - \mathcal{A}(H^*, \mathcal{D}) \leq \left(\frac{1}{2|\mathcal{D}_{te}|} \ln \frac{4n^2}{\delta}\right)^{\frac{1}{2}} \quad (4)$$

Similarly, with probability at least $(1 - \frac{\delta}{4n^2})$,

$$\mathcal{A}(H^*, \mathcal{D}) - \mathcal{A}(H^*, S_{tr}) \leq \left(\frac{1}{2|S_{tr}|} \ln \frac{4n^2}{\delta}\right)^{\frac{1}{2}} \quad (5)$$

Please note that Equation (4) and (5) will not hold if we replace H^* with $H_{S_{tr}}$. That is because for hypothesis $H_{S_{tr}}$, \mathcal{D}_{te} and S_{tr} cannot be regarded as random samples, since $H_{S_{tr}}$ is tailored to the sample set S_{tr} . Therefore, introducing H^* is necessary in our analysis.

Last, since $H_{S_{tr}}$ is trained from S_{tr} , by the fitness assumption we have:

$$\mathcal{A}(H^*, S_{tr}) - \mathcal{A}(H_{S_{tr}}, S_{tr}) \leq 0 \quad (6)$$

By substituting the four clauses in Equation (1) with Equation (3)-(6), we obtain Theorem 1 using union bound. \square

Note that the computation of $\mathcal{A}(H_{S_{tr}}, S_{tr})$ is no slower than the probing (i.e., training with sampled data). In fact, the evaluation is usually much more efficient than training for the same scale of dataset.

Lower Bound. The lower bound is easier due to the *exploitativensness* presumption discussed in the problem formulation: Full training data produce better hypothesis than sampled training data for a fixed configuration. The real test accuracy of H_{tr} can then be lower bounded by $\mathcal{A}(H_{S_{tr}}, \mathcal{D}_{te})$. However, the computation of $\mathcal{A}(H_{S_{tr}}, \mathcal{D}_{te})$ can be slower than probing, if $|\mathcal{D}_{te}| \gg |S_{tr}|$. To make the CI estimation efficient, we also sample the testing data. We denote the sampled testing data as S_{te} . We can then lower bound $\mathcal{A}(H_{S_{tr}}, \mathcal{D}_{te})$ by $\mathcal{A}(H_{S_{tr}}, S_{te})$ minus a variation term.

Theorem 2 (Lower Bound). *Under the exploitativensness assumption, with probability at least $1 - \frac{\delta}{2n^2}$,*

$$\mathcal{A}(H_{tr}, \mathcal{D}_{te}) \geq l \triangleq \mathcal{A}(H_{S_{tr}}, S_{te}) - \left(\frac{1}{2|S_{te}|} \ln \frac{2n^2}{\delta}\right)^{\frac{1}{2}}$$

Proof. First, the exploitativensness assumption states that

$$\mathcal{A}(H_{tr}, \mathcal{D}_{te}) \geq \mathcal{A}(H_{S_{tr}}, \mathcal{D}_{te}) \quad (7)$$

Next, based on Hoeffding inequality, with probability at least $1 - \frac{\delta}{2n^2}$,

$$\mathcal{A}(H_{S_{tr}}, S_{te}) - \mathcal{A}(H_{S_{tr}}, \mathcal{D}_{te}) \leq \left(\frac{1}{2|S_{te}|} \ln \frac{2n^2}{\delta}\right)^{\frac{1}{2}} \quad (8)$$

Combining Equation (7) and (8), we have $\mathcal{A}(H_{tr}, \mathcal{D}_{te}) \geq l$ with probability at least $1 - \frac{\delta}{2n^2}$. \square

With Theorem 1 and 2, we can now estimate the current lower bound and upper bound of the probing configuration C_{prob} . As shown in Algorithm 2, we first initialize the current lower bound $C_{prob.l}$ and upper bound $C_{prob.u}$ according to Theorem 1 and 2. Furthermore, we add a constraint that the current CI must be contained in the CI of the last snapshot where pruning happens, i.e., $[C_{prob.l}, C_{prob.u}] \subset [C_{prob.l_{old}}, C_{prob.u_{old}}]$. Thus, if $C_{prob.l} < C_{prob.l_{old}}$, we replace $C_{prob.l}$ with $C_{prob.l_{old}}$ (line 4). Similar for $C_{prob.u}$ (line 5). In this way, we can guarantee that the CI for each configuration shrinks from one snapshot to another snapshot where pruning happens. Recall that $C_{prob.l_{old}}$ and $C_{prob.u_{old}}$ get updated in each snapshot.

Algorithm 2: CIESTIMATOR

```

1 Input:  $C_{prob}, \mathcal{A}_{prob}(H_{S_{tr}}, S_{tr}), \mathcal{A}_{prob}(H_{S_{tr}}, S_{te})$ ;
2 Output:  $[C_{prob.l}, C_{prob.u}]$ ;
3  $[C_{prob.l}, C_{prob.u}] \leftarrow$  Theorem 1 and 2;
4 if  $C_{prob.l} < C_{prob.l_{old}}$  then  $C_{prob.l} \leftarrow C_{prob.l_{old}}$ ;
5 if  $C_{prob.u} > C_{prob.u_{old}}$  then  $C_{prob.u} \leftarrow C_{prob.u_{old}}$ ;
6 return  $[C_{prob.l}, C_{prob.u}]$ ;

```

Correctness of Algorithm 1

Theorem 3 shows that Algorithm 1 can successfully return an approximate best configuration with high probability.

Corollary 1 (Confidence Interval). *With probability at least $1 - \frac{\delta}{n^2}$, $\mathcal{A}_i \in [l_i, u_i]$.*

Theorem 3 (Correctness). *With probability at least $1 - \delta$, Algorithm 1 returns the approximate best configuration C_{i^*} with $\mathcal{A}_{i^*} - \mathcal{A}_{i'} \leq \epsilon$.*

Proof. Without loss of generality, we assume C_1 is the returned configuration $C_{i'}$ by Algorithm 1. We denote the number of snapshots as R . We will prove that when all the confidence intervals at all the snapshots correctly bound the real test accuracy (denoted as event E), the algorithm returns correct approximate configuration. We show that when E happens, for each pruned configuration $2 \leq i \leq n$, $\mathcal{A}_i \leq \mathcal{A}_1 + \epsilon$.

Consider snapshot $r \in [R]$ and let $l_{i_r}^{(r)}$ be the highest lower bound in this snapshot, and C_p be a pruned configuration in this snapshot. When E happens, $\mathcal{A}_p \leq u_p$. And $u_p \leq l_{i_r}^{(r)} + \epsilon$ according to line 9 in Algorithm 1. So the pruned configuration must satisfy $\mathcal{A}_p \leq l_{i_r}^{(r)} + \epsilon$. Furthermore, as

Algorithm 1 proceeds to snapshot $r + 1$, $l_{i_r}^{(r)} \leq l_{i_{r+1}}^{(r+1)}$. This is because the lower bound of configuration C_{i_r} does not decrease from snapshot r to snapshot $r + 1$ according to Algorithm 2, i.e., $l_{i_r}^{(r)} \leq l_{i_r}^{(r+1)}$. In addition, $l_{i_r}^{(r+1)} \leq l_{i_{r+1}}^{(r+1)}$ in snapshot $r + 1$, according to line 7 in Algorithm 1. Thus, $\mathcal{A}_p \leq l_{i_R}^{(R)} + \epsilon = l_1 + \epsilon$ by induction on the snapshot number r . Also, since $l_1 + \epsilon \leq \mathcal{A}_1 + \epsilon$, we have $\mathcal{A}_{p_r} \leq \mathcal{A}_1 + \epsilon$.

Next, let E_r be the event that all the confidence intervals at iteration r correctly bound the real test accuracy where $r \in [R]$. We can decompose event \bar{E} as $\bar{E} = \cup_{r=1}^R \bar{E}_r$, where \bar{E} (resp. \bar{E}_r) is the opposite event of E (resp. E_r). According to Corollary 1, the derived confidence interval $[l_i^{(r)}, u_i^{(r)}]$ at snapshot r is correct with probability at least $1 - \frac{\delta}{2^n}$ for any configuration C_i . Hence, the probability of \bar{E}_r is at most $\frac{\delta}{n}$ according to Algorithm 2 and the union bound. Furthermore, we have $n - 1$ pruned configurations across all iterations, so $R < n$. Consequently, the probability of \bar{E} is below δ by applying union bound to the sub-events $\bar{E}_r, r \in [R]$. That is, event E happens with probability at least $1 - \delta$. Thus, we have $\mathcal{A}_{i^*} - \mathcal{A}_{i'} \leq \epsilon$ with probability at least $1 - \delta$. \square

Discussion. Our upper confidence bound u has an additive form with three components: the training accuracy on the sampled training dataset S_{tr} , a variation term due to training sample size $|S_{tr}|$, and a variation term due to full testing data size $|D_{te}|$. Intuitively, u increases as the training accuracy $\mathcal{A}(H_{S_{tr}}, S_{tr})$ increases, because higher training accuracy indicates higher potential of the configuration's learning ability. But that potential decreases as the training sample size $|S_{tr}|$ increases, because the more data we have used, the less room for improvement by adding more training data. Finally, since the real test accuracy is measured in the full testing data D_{te} , the variation due to the random split needs to be added to u . The larger D_{te} is, the smaller the variation is. Both the variation terms are affected by the confidence probability $1 - \frac{\delta}{2^n}$. Higher confidence probability corresponds to wider confidence interval, thus larger u . In sum, u is positively correlated with the training accuracy and the number of configurations n , and negatively correlated with the training sample size and full testing data size.

Our lower confidence bound l is expressed as the accuracy of $H_{S_{tr}}$ in the sampled testing dataset S_{te} , minus a variation term due to testing sample size $|S_{te}|$. As $|S_{te}|$ increases, the difference between $\mathcal{A}(H_{S_{tr}}, S_{te})$ and $\mathcal{A}(H_{S_{tr}}, D_{te})$ becomes smaller, and the lower bound rises. Higher confidence probability $1 - \frac{\delta}{2^n}$ corresponds to smaller l . In sum, l is positively correlated with the testing sample size and the testing accuracy in the sample, and negatively correlated with n .

We have used the exploitativeness assumption in deriving the lower bound: $\mathcal{A}_i(H_{S_{tr}}, D_{te}) \leq \mathcal{A}_i(H_{tr}, D_{te})$ for any C_i . We argue that even though this assumption is not exactly satisfied in practice, it holds closely enough to provide useful results. That is, in most cases this assumption holds, and when this assumption is violated, we can perform a post-processing step after the algorithm finishes. If there exists $\mathcal{A}_{i'}(H_{S_{tr}}, D_{te}) > \mathcal{A}_{i'}(H_{tr}, D_{te})$ for the selected configuration $C_{i'}$, the user could use $H_{S_{tr}}$ instead of H_{tr} as the final classifier. First, that satisfies users' preference in finding a

more accurate classifier. Second, it holds the ϵ -guarantee, because the lower bound $l_{i'}$ holds for $H_{S_{tr}}$ of configuration $C_{i'}$, and it is no lower than the pruning lower bounds $l_{i_r}, \forall r \in [R]$.

The correctness of our algorithm is independent of the choice of the scheduler.

Scheduler

This section focuses on the optimization part in Problem 1, i.e., how to minimize the total running time. Let $T_i(s)$ be the probing time with a sampled training dataset size s for configuration C_i , and t_i be the accumulated running time for probing configuration C_i in Algorithm 1. Also, let l_i and u_i be the lower bound and upper bound respectively for configuration C_i when the algorithm terminates. With these notations, the design of SCHEDULER in ABC can be expressed as a constrained optimization problem. Without loss of generality, assume C_1 is returned by Algorithm 1.

Problem 2 (Scheduling). *Design a scheduler to minimize $\mathcal{T} = \sum_i t_i$, subject to:*

$$u_2 \leq l_1 + \epsilon, u_3 \leq l_1 + \epsilon, \dots, u_n \leq l_1 + \epsilon$$

The objective function in Problem 2 is the time taken to select the approximate best configuration. Since probing dominates the running time in each iteration, we use the total time of all probes as the proxy of the selection time. The constraints in Problem 2 ensure that all the configurations except C_1 are pruned. They are necessary for the termination of Algorithm 1.

To solve Problem 2, we begin with studying the properties of the 'oracle' optimal scheduling scheme when it has access to t_i as a function of l_i and u_i respectively, i.e., $t_i = f_i(l_i)$ and $t_i = g_i(u_i)$, after the samples are drawn. We claim that the optimal scheduling scheme with this oracle access probes each configuration uniquely once, since otherwise we can always reduce the total running time by only keeping the last probe. Our objective function can be rewritten as $f_1(l_1) + g_2(u_2) + \dots + g_n(u_n)$. Furthermore, by applying the method of Lagrange multipliers, we obtain the conditions the optimal solution must satisfy:

$$\begin{cases} \frac{df_1}{dl_1} = -\left(\frac{dg_2}{du_2} + \dots + \frac{dg_n}{du_n}\right) \\ l_1 + \epsilon = u_2 = \dots = u_n \end{cases} \quad (9)$$

Now, since we do not have oracle access to f_i and g_i , there is no closed-form formula to decide the optimal sample size s_i^* for configuration C_i . To solve this challenge, We propose a scheduling scheme GRADIENTCI with two parts.

First, we use the gradient of the running time with respect to the confidence interval to determine the configuration to probe next. We depict this strategy in Algorithm 3. GRADIENTCI first sorts the remaining configuration set Ω in descending order of the upper bound (line 3), and make a guess (Ω_1) on the best configuration C_1 . Next, it compares the gradient $\frac{\Delta T_1}{\Delta l_1}$ with $|\frac{\Delta T_2}{\Delta u_2} + \dots + \frac{\Delta T_n}{\Delta u_n}|$: If $\frac{\Delta T_1}{\Delta l_1}$ is smaller, then configuration Ω_1 with the largest upper bound is picked for the next probe (line 4); otherwise, configuration Ω_2 with

the second largest upper bound is picked (line 5). Here, ΔT_i denotes the running time difference between the recent two consecutive probes on C_i , and $\frac{\Delta T_i}{\Delta l_i}$ serves as the proxy of $\frac{\Delta f_i}{\Delta l_i}$ (similar for $\frac{\Delta g_i}{\Delta u_i}$). The choice between Ω_1 and others is based on the first condition in Equation (9). If the unit cost of increasing the lower bound of Ω_1 is smaller than the sum of the unit cost of decreasing the upper bounds of the other configurations, then we opt to probe Ω_1 . The choice of Ω_2 among Ω_2 to Ω_n is based on the second condition in Equation (9), towards attaining the same upper bound for them.

Second, we design the sample size sequence within each configuration. As shown in line 6 of Algorithm 3, we utilize a common trick called *geometric scheduling*, which was used in prior work to increase the sample size for a single configuration (Provost, Jensen, and Oates 1999). We further derive the closed-form for the optimal step size c , when $T_i(s)$ is a power function over the sample size, i.e., $T_i(s) = s^\alpha$ where α is a real number. The optimal step size follows $c = 2^{\frac{1}{\alpha}}$. Details can be found in the Appendix.

Algorithm 3: SCHEDULER-GRADIENTCI

```

1 Input: Remaining configurations  $\Omega$ ;
2 Output: Configuration for next probe  $C_{prob}$ ;
3 sort_by_upper_bound( $\Omega$ );
4 if  $\frac{\Delta T_1}{\Delta l_1} \leq |\frac{\Delta T_2}{\Delta u_2} + \dots + \frac{\Delta T_n}{\Delta u_n}|$  then  $C_{prob} \leftarrow \Omega_1$ ;
5 else  $C_{prob} \leftarrow \Omega_2$ ;
6  $C_{prob} \cdot s \leftarrow c \times C_{prob} \cdot s$ ;
7 return  $C_{prob}$ ;

```

Performance Analysis. In practice, ABC is used in two scenarios. Scenario (i): during exploration, users want to try a few configurations (e.g., verifying usefulness of a few new features) as an intermediate step. The best configuration will decide the follow-up trials, but it does not serve as the final configuration, and does not require full training. Scenario (ii): at the end of the exploration, users need to get the trained classifier corresponding to the selected configuration $C_{i'}$. In scenario (ii), the total running time involves not only the time to select the approximate best configuration, but also the time taken to train the classifier on full data with $C_{i'}$. When $C_{i'}$ is fixed, both scenario (i) and (ii) share the same optimal scheduler. Under certain conditions, we are able to prove a 4-approx guarantee for GRADIENTCI. Please find details in the Appendix.

Remark. We have also analyzed a well-known scheduling scheme, called UCB. Theoretical and experimental results can be found in the Appendix.

Experiments

This section evaluates the efficiency and effectiveness of our ABC module. First, we evaluate whether ABC successfully selects top configuration and meanwhile reduces the total running time. Second, we compare the CI-based pruning with an existing pruning algorithm based on point estimation. We also compare different scheduling schemes in the Appendix.

Experimental Setup

Configurations. We focus on the task of classifying featurized data in our evaluation. Specifically, we choose five widely used and high-performance learners: *LogisticRegression*, *LinearSVM*, *LightGBM*, *NeuralNetwork*, and *RandomForest*. Each classifier is associated with various hyperparameters, e.g., the number of trees in RandomForest and the penalty coefficient in LinearSVM. In total they have 29 discrete or continuous hyperparameters. In our experiments, we use random search to generate each hyperparameter value from its corresponding domain.

Datasets. We evaluate with five large-scale machine learning benchmarks that are publicly available. As discussed in introduction, the motivation of ABC is to handle large datasets and quickly select the approximate best configuration. Thus, the datasets evaluated in our experiments are all at the scale of millions of records ($|\mathcal{D}|$) and with up to 10K features ($|\mathcal{F}|$). We do not use the AutoML benchmarks such as HPOlib (Eggenberger et al. 2013) or OpenML (Vanschoren et al. 2013), which mainly contain small or median-sized datasets (up to 50K records). The statistics of each dataset are depicted in Table 2. We used min-max normalization for all datasets, and n-gram extraction as well as model-based top-K feature selection for Twitter. The processed datasets are available from <https://www.microsoft.com/en-us/research/people/chiw/#!downloads>.

Algorithms. We compare our proposed ABC with the standard approach named *Full-run*. For each configuration, Full-run first trains the classifier with full training data, and then tests it on the full testing data. Afterwards, it returns the configuration with the highest testing accuracy. This method is supported in mature tools like scikit-learn and Azure ML. Existing approaches to best configuration selection, such as DAUB (Sabharwal, Samulowitz, and Tesauro 2016) or Successive-halving (Jamieson and Talwalkar 2016), are heuristics without accuracy guarantee. Our solution and such heuristics are not apple-to-apple comparison, as they cannot ensure ϵ -approximation guarantee on accuracy. Nevertheless, we conduct a best effort comparison with them.

Setup. We conducted our evaluation on a VM with 8 cores and 56 GB RAM. The initial training sample size and testing sample size are 1000 and 2000 respectively. The geometry step size is set to be $c = 2$. $\epsilon = 0.01, \delta = 0.5$. Since δ is under the log term, the result is not sensitive to δ . We also conduct experiments with varying ϵ , as shown in the Appendix.

We use the same set of sampled configurations for both Full-run and ABC. We vary the number of input configurations from 5 to 80. Since we focus on large datasets, it already takes a day or half to finish Full-run with 80 configurations for a single dataset. So unlike the case of small datasets, 80-100 is a realistic number because that is how many configurations a user can try with Full-run within a reasonable period of waiting.

ABC vs. Full-run

We compare ABC against Full-run from two perspectives, running time and accuracy. We first compute the *speedup*

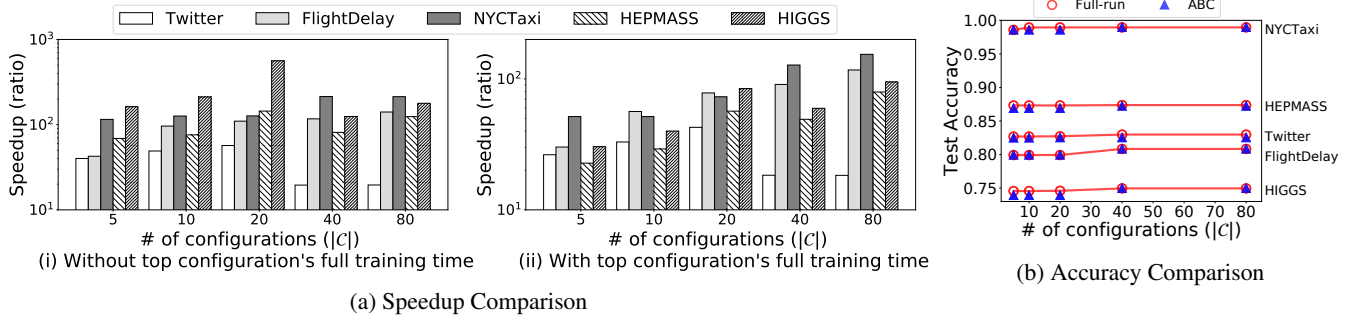


Figure 3: Comparison Between Full-run and ABC

achieved by ABC, where speedup is defined as the ratio between Full-run’s total running time and ours. Next, we compare the configuration $C_{i'}$ returned by our ABC with the best configuration C_{i^*} provided by Full-run in terms of real test accuracy.

Efficiency Comparison. As discussed, ABC is used in two scenarios in practice. During exploration, users only need the selected configuration to decide the follow-up trials, but do not require full training with the selected configuration. At the end of the exploration, users need to train the classifier with the selected configuration in the full data. Thus, we evaluate the running time speedup in these two scenarios: (i) we first compare the selection time between our ABC and Full-run as depicted in Figure 3a(i); (ii) we then compare the total running time including the time to train the final classifier, in Figure 3a(ii). Our solution is on average $190\times$ faster than Full-run in scenario (i), and is on average $60\times$ faster than Full-run in scenario (ii). Furthermore, 23 out of 25 experiments (i.e., 5 different datasets times 5 different configuration set size) has at least $|\mathcal{C}|\times$ speedup in scenario (i), and 22 out of 25 experiments achieve at least $|\mathcal{C}|\times$ speedup in scenario (ii). This means that the running time of ABC is even faster than fully evaluating one average configuration in most cases, which further means even a perfectly distributed Full-run can’t beat the non-distributed ABC.

The speedup on dataset Twitter is consistently lower than other datasets. This is mainly because Twitter is one order of magnitude smaller than the other datasets. With the same sample size, the sampling ratio is higher than the other datasets, which causes lower speedup.

Effectiveness Comparison. As illustrated in Figure 3b, ABC successfully selects the configuration whose real test accuracy is within 0.01 from the best configuration’s real test accuracy in all of our experiments. In particular, when $|\mathcal{C}| = 40$ or 80, ABC successfully identifies the exact best configuration for FlightDelay, NYCTaxi, and HIGGS. The largest deviation is around 0.0068 when $|\mathcal{C}| = 20$ for HIGGS.

Takeaway. Compared to Full-run, our proposed ABC can successfully select a competitive or identical best configuration but with much less time.

CI-based Pruning vs. Successive-halving

Next, we compare our proposed CI-based pruning with Successive-halving. Successive-halving was proposed as a pruning strategy to evaluate iterative training configurations with a resource budget of the total number of iterations of all configurations. We modify it to use the total sample size as the resource budget. In each round, it trains a classifier with the sampled data for each remaining configuration, and then eliminates the half of the low-performing configurations. This pruning is based on point estimation, i.e., they directly use $\mathcal{A}(H_{S_{tr}}, D_{te})$ to approximate $\mathcal{A}(H_{tr}, D_{te})$, in contrast to using confidence interval as ABC. It repeats until there is only one remaining configuration.

Since the two solutions are designed to satisfy different constraints (accuracy loss and resource), they are not directly comparable. We do our best to make a fair comparison. In this section, we run Successive-halving with identical sample size sequence as ABC, to compare the CI-based pruning and the halving strategy based on point estimation. We perform the same set of experiments as in the previous experiment section for Successive-halving. We introduce a metric, called *relative accuracy loss*, to measure the difference between the returned configuration $C_{i'}$ and the best configuration C_{i^*} in terms of the test accuracy: $\Delta_{rel} = \frac{|A_{i^*} - A_{i'}|}{A_{i^*}}$. The smaller Δ_{rel} is, the better.

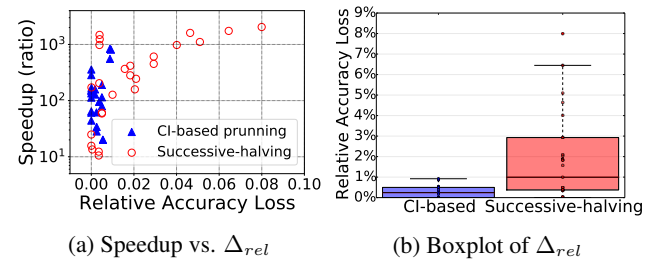


Figure 4: ABC vs. Successive-halving

We depict the comparison between Successive-halving and our ABC in Figure 4. The x-axis in Figure 4a refers to the relative accuracy loss compared to the best configuration by Full-run, the y-axis is the speedup compared to the running time of Full-run, and each point corresponds to a specific

experiment with a certain dataset and C . We can see that Successive-halving has a similar speedup as ABC over Full-run. However, the relative accuracy loss can be an order of magnitude larger than that of ABC, e.g., 8% vs. 0.8%. This is because the pruning performed in Successive-halving is based on the ranking of the current test accuracy. On the contrary, ABC uses confidence interval of the real test accuracy to perform safer pruning. Figure 4b presents a boxplot summarizing the relative accuracy loss for our solution and Successive-halving respectively. On average, the relative accuracy loss for our CI-based solution is 0.24% (all below 1%), and 2% for Successive-halving (up to 8%), which is nearly ten times larger. In order to fully compare Successive-halving and our ABC, we have also conducted another set of experiments with varying time constraint. The results can be found in the Appendix. In addition, we report the performance of an enhanced algorithm of DAUB using our CIEstimator and CI-based pruning in the Appendix.

Related Work

AutoML. AutoML has gained increasing attention in the past few years. The scope of AutoML includes automated feature engineering, model selection, and hyperparameter tuning process. Some prevailing AutoML tools are Auto-sklearn for Python (Feurer et al. 2015) and Auto-Weka for Java (Thornton et al. 2013). Most research focus is devoted to the search strategy, i.e., which configurations to evaluate. The strategies can be broadly categorized as grid search (Pedregosa et al. 2011), random search (Bergstra and Bengio 2012), spectral search (Hazan, Klivans, and Yuan 2018), Bayesian optimization (Hutter, Hoos, and Leyton-Brown 2011; Bergstra et al. 2011; Snoek, Larochelle, and Adams 2012), meta-learning (Feurer et al. 2015), and genetic programming (Olson et al. 2016). Few studies address the efficiency issue in ranking these configurations on large datasets. TuPAQ (Sparks et al. 2015) and HyperDrive (Rasley et al. 2017) are two systems which focus on hyperparameter tuning when all the configurations correspond to iterative training processes. They distribute the configurations into multiple machines, and use heuristic early stopping rules for training iterations. (Jamieson and Talwalkar 2016) further models this problem as a non-stochastic multi-armed bandit process, where each arm corresponds to a configuration, each pull corresponds to a few training iterations, and the reward is the intermediate accuracy on the test data. Recognizing the difference with the stochastic bandit process, they propose a Successive-halving pruning strategy in the fixed budget setting. They focus on this setting because they have found it difficult to derive the confidence bounds of real test accuracy based on limited training iterations. Hyperband (Li et al. 2017) uses Successive-halving as a building block and tries to vary the number of random configurations under the same budget. While Hyperband suggests that the notion of resource can be generalized from training iterations to sample size of training data, we should notice that it is now possible to derive confidence bounds of real test accuracy based on sampled training data. Therefore, ABC can be used to replace Successive-halving in this scenario to achieve lower accuracy loss. In the Bayesian optimization framework, RoBO (Klein

et al. 2017) treats the sample size as a hyperparameter, and uses random sample size to evaluate each configuration and a kernel function to extrapolate the real test accuracy.

Generalization Error Bounds. Generalization error bound has been studied extensively (Zhou 2002; Koltchinskii et al. 2000; Bousquet and Elisseeff 2002), among which *VC-bound* (Vapnik 1999) is a well-known technique for bounding the generalization error. The main idea behind VC-bounds is to use *VC-dimension* to characterize the complexity of the hypothesis class. Besides VC-dimension, other existing techniques for deriving generalization error bounds include covering number (Zhou 2002), Rademacher complexity (Koltchinskii et al. 2000), and stability bound (Bousquet and Elisseeff 2002). While the definition of generalization error bounds is different from the confidence bound needed for ABC, they have been used in other work to guide progressive sampling for a *single* configuration (Elomaa and Kääriäinen 2002).

Discussion and Conclusion

We studied the problem of efficiently finding approximate best configuration among a given set of training configurations for a large dataset. Our CI-based progressive sampling and pruning solution ABC can successfully select a top configuration with small or no accuracy loss, in much less time than the exact approach. The CI-based pruning is more robust than pruning based on point estimates.

There are multiple use cases that can benefit from our proposed ABC. The input of ABC can be either specified by the users based on their domain knowledge, or generated from an AutoML search algorithm. Our ABC module can help data scientists select a top configuration faster. As they iteratively refine it, they can use ABC to verify whether altering part of the configuration (such as changing features) boosts the performance, by invoking ABC with the old and new configurations. In addition, our confidence bounds can be potentially used to accelerate Bayesian optimization and spectral search in large datasets, which is interesting future work.

References

- [Bergstra and Bengio 2012] Bergstra, J., and Bengio, Y. 2012. Random search for hyper-parameter optimization. *Journal of Machine Learning Research* 13(Feb):281–305.
- [Bergstra et al. 2011] Bergstra, J. S.; Bardenet, R.; Bengio, Y.; and Kégl, B. 2011. Algorithms for hyper-parameter optimization. In *NIPS'11*.
- [Bousquet and Elisseeff 2002] Bousquet, O., and Elisseeff, A. 2002. Stability and generalization. *Journal of machine learning research* 2(Mar):499–526.
- [Eggenberger et al. 2013] Eggenberger, K.; Feuerer, M.; Hutter, F.; Bergstra, J.; Snoek, J.; Hoos, H.; and Leyton-Brown, K. 2013. Towards an empirical foundation for assessing bayesian optimization of hyperparameters. In *NIPS workshop on Bayesian Optimization in Theory and Practice*.
- [Elomaa and Kääriäinen 2002] Elomaa, T., and Kääriäinen, M. 2002. Progressive rademacher sampling. In *AAAI'02*.
- [Feurer et al. 2015] Feuerer, M.; Klein, A.; Eggenberger, K.; Springenberg, J.; Blum, M.; and Hutter, F. 2015. Efficient and robust automated machine learning. In *NIPS'15*.

[Hazan, Klivans, and Yuan 2018] Hazan, E.; Klivans, A.; and Yuan, Y. 2018. Hyperparameter optimization: A spectral approach. In *ICLR'18*.

[Hutter, Hoos, and Leyton-Brown 2011] Hutter, F.; Hoos, H. H.; and Leyton-Brown, K. 2011. Sequential model-based optimization for general algorithm configuration. In *International Conference on Learning and Intelligent Optimization*.

[Jamieson and Talwalkar 2016] Jamieson, K., and Talwalkar, A. 2016. Non-stochastic best arm identification and hyperparameter optimization. In *AISTATS'16*.

[Klein et al. 2017] Klein, A.; Falkner, S.; Mansur, N.; and Hutter, F. 2017. Robo: A flexible and robust bayesian optimization framework in python. In *NIPS 2017 Bayesian Optimization Workshop*.

[Koltchinskii et al. 2000] Koltchinskii, V.; Abdallah, C. T.; Ariola, M.; Dorato, P.; and Panchenko, D. 2000. Improved sample complexity estimates for statistical learning control of uncertain systems. *IEEE Transactions on Automatic Control* 45(12):2383–2388.

[Li et al. 2017] Li, L.; Jamieson, K.; DeSalvo, G.; Rostamizadeh, A.; and Talwalkar, A. 2017. Hyperband: A novel bandit-based approach to hyperparameter optimization. In *ICLR'17*.

[Olson et al. 2016] Olson, R. S.; Bartley, N.; Urbanowicz, R. J.; and Moore, J. H. 2016. Evaluation of a tree-based pipeline optimization tool for automating data science. In *Proceedings of the Genetic and Evolutionary Computation Conference 2016, GECCO'16*.

[Pedregosa et al. 2011] Pedregosa, F.; Varoquaux, G.; Gramfort, A.; Michel, V.; Thirion, B.; Grisel, O.; Blondel, M.; Prettenhofer, P.; Weiss, R.; Dubourg, V.; Vanderplas, J.; Passos, A.; Cournapeau, D.; Brucher, M.; Perrot, M.; and Duchesnay, E. 2011. Scikit-learn: Machine learning in python. *JMLR* 12:2825–2830.

[Provost, Jensen, and Oates 1999] Provost, F.; Jensen, D.; and Oates, T. 1999. Efficient progressive sampling. In *KDD'99*.

[Rasley et al. 2017] Rasley, J.; He, Y.; Yan, F.; Ruwase, O.; and Fonseca, R. 2017. Hyperdrive: Exploring hyperparameters with pop scheduling. In *Proceedings of the 18th ACM/IFIP/USENIX Middleware Conference*.

[Sabharwal, Samulowitz, and Tesauro 2016] Sabharwal, A.; Samulowitz, H.; and Tesauro, G. 2016. Selecting near-optimal learners via incremental data allocation. In *AAAI'16*.

[Snoek, Larochelle, and Adams 2012] Snoek, J.; Larochelle, H.; and Adams, R. P. 2012. Practical bayesian optimization of machine learning algorithms. In *NIPS'12*.

[Sparks et al. 2015] Sparks, E. R.; Talwalkar, A.; Haas, D.; Franklin, M. J.; Jordan, M. I.; and Kraska, T. 2015. Automating model search for large scale machine learning. In *Proceedings of the Sixth ACM Symposium on Cloud Computing*.

[Thornton et al. 2013] Thornton, C.; Hutter, F.; Hoos, H. H.; and Leyton-Brown, K. 2013. Auto-weka: Combined selection and hyperparameter optimization of classification algorithms. In *KDD'13*.

[Vanschoren et al. 2013] Vanschoren, J.; van Rijn, J. N.; Bischl, B.; and Torgo, L. 2013. Openml: Networked science in machine learning. *SIGKDD Explorations* 15(2):49–60.

[Vapnik 1999] Vapnik, V. N. 1999. An overview of statistical learning theory. *IEEE transactions on neural networks* 10(5):988–999.

[Zhou 2002] Zhou, D.-X. 2002. The covering number in learning theory. *Journal of Complexity* 18(3):739–767.

Appendices

Optimal Step Size in Geometric Scheduling

When $T_i(s)$ is a power function over the sample size, i.e., $T_i(s) = s^\alpha$ where α is a real number, the optimal step size follows $c = 2^{\frac{1}{\alpha}}$.

Proof. Assume s_i^* is the *optimal* training sample size for each configuration C_i when Algorithm 1 terminates. As we do not know the optimal s_i^* in advance, we try probes with progressive sample size for each configuration C_i , denoted as $\{s_i^1, s_i^2, \dots, s_i^m\}$, where s_i^m is the sample size in the last probe of C_i when Algorithm 1 terminates. For a fixed i , we assume that the last probe of all the other configurations uses their optimal training sample size, i.e., $s_{i'}^m = s_{i'}^*, \forall i' \neq i$. Thus, the termination point for C_i must satisfy (a) $s_i^m \geq s_i^*$, otherwise s_i^m would be a smaller sample size for configuration C_i than s_i^* ; and (b) $s_i^{m-1} < s_i^*$, otherwise Algorithm 1 would terminate at s_i^{m-1} instead of s_i^m .

Based on the above property, we first claim that with geometric schedule (i.e., $s_i^j = c^{j-1}s_i^1$, where s_i^1 is the sample size in the initial probe and c is the geometric step size), the accumulated running time is asymptotically equivalent to the optimal running time (i.e., $\sum_{j=1}^m T_i(s_i^j) = \mathcal{O}(T_i(s_i^*))$) (Provost, Jensen, and Oates 1999). Recall that $T_i(s) = s^\alpha$ is the probing time with a sampled training dataset of size s for configuration C_i .

We further minimize the worst case ratio between the accumulated running time and the optimal running time, i.e., $\frac{\sum_{j=1}^m T_i(s_i^j)}{T_i(s_i^*)}$. Since $s_i^{m-1} < s_i^* \leq s_i^m$, the worst case occurs when $s_i^* = s_i^{m-1}$. By replacing each term $T_i(s)$ with s^α and solving $\min_c \frac{\sum_{j=1}^m T_i(s_i^j)}{T_i(s_i^{m-1})}$, we can derive a closed form solution for c . When the step size follows $c = 2^{\frac{1}{\alpha}}$, $\frac{\sum_{j=1}^m T_i(s_j)}{T_i(s_i^{m-1})}$ is minimized and it is guaranteed that $\frac{\sum_{j=1}^m T_i(s_j)}{T_i(s_i^*)} \leq 4$ in any case. For instance, when the training time $T_i(s)$ increases linearly with the sample size s , i.e., $\alpha = 1$, then we should set c to 2, which means we should double the sample size as the probing proceeds for each configuration. In fact, Provost et.al. (Provost, Jensen, and Oates 1999) set $c = 2$ heuristically and found good empirical performance. Our analysis provides a theoretical justification for that heuristic. \square

Performance Analysis of GRADIENTCI

It is hard to bound the performance of GRADIENTCI in general cases. However, under certain conditions, we are able to prove a 4-approx guarantee for GRADIENTCI with respect to the oracle optimal running time when $\epsilon = 0$ for the scenario where users need to get the trained classifier corresponding to the selected configuration $C_{i'}$. Remember that in this scenario, the total running time involves both the time to select the approximate best configuration, and the time taken to train the classifier on full data with $C_{i'}$.

Assumption 1 (CI Condition). *All confidence intervals correctly bound the test accuracy and shrink as Algorithm 1 proceeds.*

Assumption 2 (Convex Condition). *f_i and g_i are convex functions of l_i and u_i respectively.*

Assumption 3 (Proxy Condition). *For $C_i \in \mathcal{C}$, $\frac{\Delta f_i}{\Delta l_i} = \frac{\Delta T_i}{\Delta l_i}$ and $\frac{\Delta g_i}{\Delta u_i} = \frac{\Delta T_i}{\Delta u_i}$.*

First, CI Condition means that we only focus on the case where all the confidence intervals correctly bound the test accuracies. In this case, for each configuration, its lowest upper bound and highest lower bound in all the rounds still bound the real test accuracy correctly, and the upper (lower, resp.) bound is monotonically decreasing (increasing, resp.) as Algorithm 1 runs. Second, the convex condition means that the increase of sample size has a diminishing return to the change of the CI – as Algorithm 1 proceeds, it takes longer to attain the same increase (decrease, resp.) on the lower bound (upper bound, resp.). Last, since the gradient $\frac{\Delta f_i}{\Delta l_i}$ ($\frac{\Delta g_i}{\Delta u_i}$, resp.) is impossible to compute, we can only use $\frac{\Delta T_i}{\Delta l_i}$ ($\frac{\Delta T_i}{\Delta u_i}$, resp.) to approximate it. The proxy condition means such approximation is accurate and effective.

Theorem 4 (GRADIENTCI 4-Approx). *Under Assumption 1 to 3, GRADIENTCI provides a 4-approx guarantee to the oracle optimal running time to get the final trained classifier when $\epsilon = 0$.*

Proof. We illustrate our analysis with the help of Figure 5. Without loss of generality, we consider C_1 as the best configuration C_{i^*} . Each vertical line corresponds to one configuration, with shrinking confidence intervals as Algorithm 1 proceeds according to the CI condition. The red and blue lines with the same length depict a corresponding pair of upper and lower bound after a particular probe in Algorithm 1. Let $l^* = u^*$ be the optimal solution in Equation (9), as shown by the solid horizontal black line in Figure 5. Furthermore, as shown in Figure 5, let l_1^* be the smallest lower bound of C_1 that is larger than l^* , and u_i^* be the largest upper bound of C_i that is smaller than u^* , where $2 \leq i \leq n$. In the following, we prove that with our proposed scheduling scheme GRADIENTCI, for each configuration C_i , $2 \leq i \leq n$, the upper confidence bound cannot cross below the red solid line u_i^* in Figure 5, i.e., Algorithm 1 terminates with $u_i \geq u_i^*$.

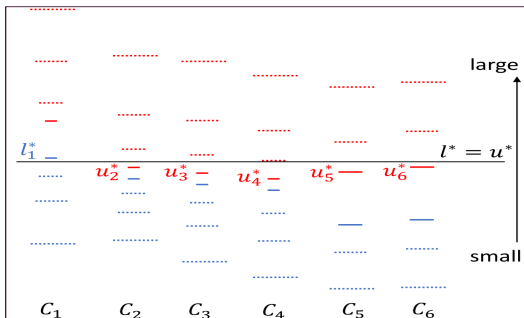


Figure 5: Analysis of GRADIENTCI

For any $2 \leq i \leq n$, we will prove by induction that $u_i \geq u_i^*$ at every iteration of Algorithm 1. First, it is obvious that in the first iteration (or probe), $u_i \geq u_i^*$ for any $2 \leq i \leq n$. Next, suppose $u_i \geq u_i^*$ after the $(k-1)^{th}$ iteration of Algorithm 1, we will show that $u_i \geq u_i^*$ after the k^{th} iteration for any $2 \leq i \leq n$ and $k \geq 2$. Since one probe is performed in each iteration, we only need to prove that for the probing configuration C_{prob} , $u_{prob} \geq u_{prob}^*$ still holds when $C_{prob} \neq C_1$. Recall that in each iteration, GRADIENTCI makes the guess that the configuration with largest upper bound is the best configuration. In the following, we discuss two cases depending on whether that guess is right in the k^{th} iteration. For notation simplicity, let C_j be the probing configuration C_{prob} in the k^{th} iteration.

Case 1. GRADIENTCI has a wrong guess of the best configuration C_1 . Suppose $C_{i'}$ is speculated as the best configuration. By definition, $u_{i'} \geq u_1 \geq \mathcal{A}_1 \geq l^* > u_{i'}^*$. Hence, if the probing configuration C_j is $C_{i'}$, then we have shown that $u_j > u_j^*$. Otherwise, the probing configuration C_j must be the one with the second highest upper bound, according to GRADIENTCI. In that case, $u_j \geq u_1$ since C_1 is also compared against when identifying the configuration with second highest upper bound, and $u_1 \geq \mathcal{A}_1 \geq l^* > u_j^*$ by definition. Thus, $u_j > u_j^*$. Now we have shown that $u_j > u_j^*$ at the beginning of the k^{th} iteration. Thus, we have $u_j \geq u_j^*$ after the k^{th} iteration due to the one probe on C_j .

Case 2. GRADIENTCI has a correct guess on C_1 . If C_1 is probed, then we are done since u_i does not change for $2 \leq i \leq n$. Otherwise, the probing configuration C_j is the one with the second highest upper bound, according to GRADIENTCI. In that case, we prove $u_j \geq u_j^*$ after the k^{th} iteration by contradiction. If $u_j < u_j^*$ after the k^{th} iteration, then u_j must equal u_j^* at the beginning of the k^{th} iteration since we assume $u_j \geq u_j^*$ holds after the $(k-1)^{th}$ iteration. Next, we will show $u_i = u_i^*$ at the beginning of the k^{th} iteration for all $2 \leq i \leq n$ and $i \neq j$.

First, for $2 \leq i \leq n$, $i \neq j$, and $u_i \in \Omega$ at the beginning of the k^{th} iteration in Algorithm 1, u_i must equal u_i^* , since otherwise C_j can not be with the second highest upper bound. Recall the Ω is the remaining candidate configurations. Second, for $2 \leq i \leq n$, $i \neq j$, and $u_i \notin \Omega$, we will show C_i must have been pruned when u_i equals u_i^* , by contradiction. Otherwise (i.e., $u_i > u_i^*$), $u_i \geq u^*$ and C_j is thus pruned before the k^{th} iteration since $u_j = u_j^* < u^* \leq u_i$, which contradict with the fact that $C_j \in \Omega$.

Hence, we have $u_i = u_i^*$ at the beginning of the k^{th} iteration for all $2 \leq i \leq n$. Thus, $l_1 < l^*$, since otherwise all the other configurations are pruned. As a consequence, we have $\frac{df_1}{dl_1} \leq |\frac{dg_2}{du_2} + \dots + \frac{dg_n}{du_n}|$, since $\frac{df_1}{dl_1}$ decreases with the decrease of l_1 and $|\frac{dg_i}{du_i}|$ increases with the decrease of u_i according to the convex condition. Then based on GRADIENTCI, C_1 should be probed, which contradicts with the assumption that the probing configuration C_j is with the second highest upper bound. Altogether, $u_j \geq u_j^*$ for case 2.

Combining case 1 and case 2, we now have shown that when Algorithm 1 terminates, $u_i \geq u_i^*$, $\forall 2 \leq i \leq n$. Equiva-

lently speaking, each configuration C_i ($2 \leq i \leq n$) is probed at most one more time compared to the optimal scheme (the solid horizontal black line in Figure 5). In addition, given a configuration, each probe’s running time is twice of that in its previous probe, since we have set $c^\alpha = 2$. Thus, the accumulated running time of GRADIENTCI is at most 4 times of the optimal runtime for any configuration C_i , where $2 \leq i \leq n$. That is:

$$t_i \leq 4t_i^*, \forall 2 \leq i \leq n$$

where t_i^* is the optimal running time corresponding to the optimal scheme for identifying the best configuration and t_i is the accumulated running time for C_i in GRADIENTCI. In the worst case, C_1 is probed all the way till with full training data. With $c^\alpha = 2$, we have $t_1 \leq 2T_1(|\mathcal{D}_{tr}|)$.

Recall that in the scenario where users need to get the final trained classifier, the total running time has two terms: the time taken to select the approximate best configuration and the time to get the trained classifier corresponding to the selected configuration (i.e., $\mathcal{T} = \sum_i t_i + T_1(|\mathcal{D}_{tr}|)$). Since $\mathcal{T}_{min} = \sum_{i=1}^n t_i^* + T_1(|\mathcal{D}_{tr}|)$ and $\mathcal{T} = \sum_{i=1}^n t_i + T_1(|\mathcal{D}_{tr}|)$, we have $\mathcal{T} \leq 4\mathcal{T}_{min}$. \square

UCB as Scheduler

Upper Confidence Bound (UCB) is a common scheduling scheme in multi-armed bandit problem. To apply UCB to our problem, in each iteration we always pick the configuration with the highest upper confidence bound for probing. The intuition is that the upper bound reflects the potential of this particular configuration, and thus the configuration with higher upper bound deserves more exploration. UCB tries to push down the highest upper bound, which kind of matches the second condition in Equation (9). However, UCB does not take lower bound’s growth rate and upper bound’s decrease rate into consideration, i.e., the first condition in Equation (9). Intuitively, when the configuration with the highest upper bound takes a long time for probing but the confidence interval shrinkage is only marginal, we should opt for probing other configurations. Motivated by this, our proposed SCHEDULER, i.e., GRADIENTCI, have taken the potential (i.e., upper bound), together with the upper bound’s decrease rate and the lower bound’s growth rate into consideration.

To compare the gradient-based approach (i.e., GRADIENTCI) with UCB, we also apply geometric scheduling within each configuration for UCB. Under certain conditions, we are able to show a $4\times$ approximation guarantee for UCB in Theorem 5 when $\epsilon = 0$.

Theorem 5 (UCB Approx Guarantee). *Under Assumption 1, UCB provides a 4-approx guarantee to the optimal running time to get the final trained classifier when $\epsilon = 0$.*

Proof. Similar to the proof in Theorem 4, we use Figure 5 to help illustrate the analysis. In the following, we prove that with UCB, for each configuration C_i , $2 \leq i \leq n$, the upper confidence bound cannot cross below the red solid line u_i^* in Figure 5, i.e., Algorithm 1 terminates with $u_i \geq u_i^*$.

For any $2 \leq i \leq n$, we will prove *by induction* that $u_i \geq u_i^*$ at every iteration of Algorithm 1. First, it is obvious

that in the first iteration (or probe), $u_i \geq u_i^*$ for any $2 \leq i \leq n$. Next, suppose $u_i \geq u_i^*$ after the $(k-1)^{th}$ iteration of Algorithm 1, we will show that $u_i \geq u_i^*$ after the k^{th} iteration for any $2 \leq i \leq n$ and $k \geq 2$. Since one probe is performed in each iteration, we only need to prove that for the probing configuration C_{prob} , $u_{prob} \geq u_{prob}^*$ still holds when $C_{prob} \neq C_1$. For notation simplicity, let C_j be the probing configuration C_{prob} in the k^{th} iteration.

We prove it *by contradiction*. If $u_j < u_j^*$ after the k^{th} iteration. then u_j must equal u_j^* at the beginning of the k^{th} iteration since we assume $u_j \geq u_j^*$ holds after the $(k-1)^{th}$ iteration. That is, $u_j = u_j^* < u_j^*$. Based on the confidence interval property, we know that $u^* = l^* \leq \mathcal{A}_1 \leq u_1$. Hence, we have $u_j < u_1$, which contradicts with the fact that C_j is with the highest upper bound and is selected as the probe configuration.

Thus, we proved that each configuration probes at most one more time than the optimal scheme, i.e., $u_i \geq u_i^*$ where $2 \leq i \leq n$. The remainder of the proof is the same as in Theorem 4. \square

Extra Experiments

Varying ϵ in CI-based Framework

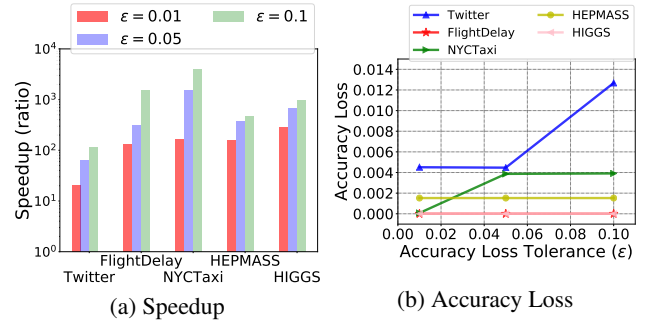


Figure 6: Speedup vs. Accuracy Loss with Varying ϵ

In this experiment, we compare the real accuracy loss and the speedup with varying input accuracy loss tolerance ϵ . As shown in Figure 6, with the increase of the input ϵ , both the speedup and the real accuracy loss increase. First, as ϵ increases, the pruning condition is easier to be satisfied, leading to faster termination of Algorithm 1. Second, with smaller running time (i.e., resource) on each configuration, the CIESTIMATOR tends to be less accurate. Consequently, the real accuracy loss typically increases as the increase of ϵ . As depicted in Figure 6b, the real accuracy loss increases slightly as ϵ increases. Specifically, when $\epsilon = 0.1$, the real accuracy loss is 0.012 for Twitter, and below 0.004 for other datasets, while the speedup reaches 3 orders of magnitude for FlightDelay, NYCTaxi, and HIGGS.

Varying Time Constraint in CI-based Pruning vs. Successive-halving

In addition to the scenario of no resource constraint in the main paper, we also study the performance of our CI-based

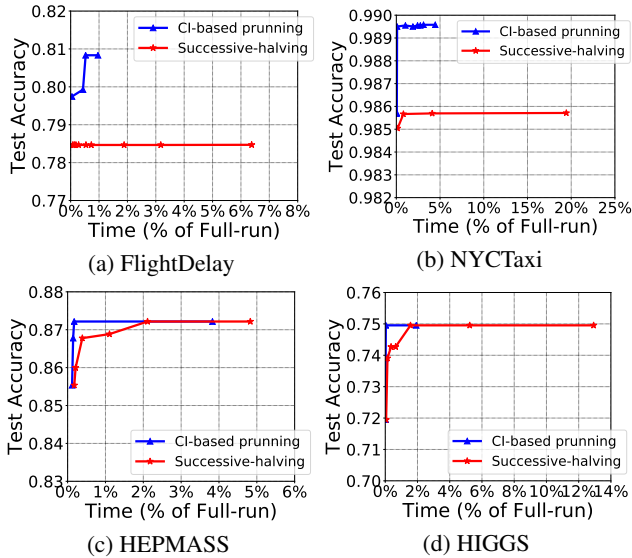


Figure 7: CI-based Pruning vs. Successive-halving with Varying Time Constraint

framework and Successive-halving, when we impose resource constraint on these two algorithms. In general, our CI-based framework dominates Successive-halving with varying resources, i.e., with the same resource, our framework returns the configuration with higher testing accuracy than that provided by Successive-halving.

For Successive-halving, the resource budget is controlled by the initial sample size. We vary the initial training sample size in Successive-halving starting from 250 and increase the initial training sample size by 2 every time. The initial test sample size is always twice of the initial training sample size. Each point in the red line of Figure 7 corresponds to one initial sample size, and the left most point has 250 initial training samples. As a result, we can attain various running time of Successive-halving, and we further normalize them as the percentage of Full-run’s running time. For our CI-based framework, we add the option for it to terminate at any iteration. In Algorithm 1, we output a best-guess configuration at the end of each iteration. Specifically, we compare the configuration $C_{\mathcal{V}}$ (with the highest lower bound so far) against the configuration Ω_1 (with the highest upper bound so far), and output the one with smaller gap between its lower bound and the highest upper bound of all the other configurations. The intuition is that, in order to prune all the other configurations, we need to compare the lower bound of the output configuration with the upper bound of all the other configurations, and we would like this gap to be as small as possible such that the bound of the accuracy loss between the output configuration and the best configuration is small. Each point in the blue line of Figure 7 corresponds to one such best-guess configuration.

In Figure 7, x-axis is the running time percentage taken compared to Full-run, and y-axis is the real test accuracy for the returned configuration. From Figure 7, we can see that our CI-based framework dominates Successive-halving. In particular, the test accuracy provided by Successive-halving

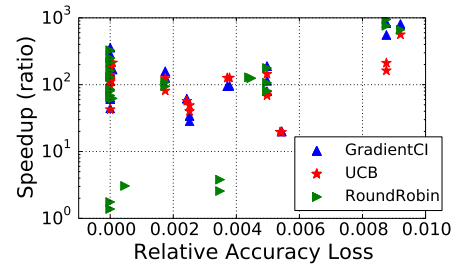


Figure 8: Comparison of Different Scheduling Schemes

is much worse than that returned by our framework in Figure 7(a)(b); while in Figure 7(c)(d) Successive-halving takes much longer time to reach the same test accuracy as that in our framework. In general, when starting with larger initial training sample size, Successive-halving can return better configuration. This is because the point estimation in Successive-halving is more accurate when using larger training sample size. However, this in turn increases the total running time of Successive-halving, making it inferior to our CI-based framework. The result suggests that the ABC is also useful in the resource-constrained scenario, though it was not designed for that scenario.

Comparison of Scheduling Schemes

Within the CI-based framework ABC, we now empirically study the impact of three different scheduling schemes, i.e., GRADIENTCI, UCB, and ROUNDROBIN.

Recall that UCB always picks the configuration with the highest upper confidence bound for probing. ROUNDROBIN allocates resources (i.e., probes) evenly among the remaining configurations. Specifically, ROUNDROBIN chooses the configuration with the smallest number of probes as the C_{prob} in each iteration, replacing line 10 in Algorithm 1.

We perform the same set of experiments as that in the main experiment section, but with different scheduling schemes in our CI-based framework. First, we observe that in most cases, when applying different scheduling schemes, the accuracy loss of the returned configuration remains almost the same. However, the speedup differs from GRADIENTCI to UCB and ROUNDROBIN. Figure 8 depicts the speedup and relative accuracy loss achieved by different scheduling schemes. Each point refers to a particular dataset and a configuration set size $|\mathcal{C}|$. With the same relative accuracy loss, GRADIENTCI can achieve the highest speedup in most cases. We notice that ROUNDROBIN performs much more slowly in a few cases (speedup below 5 while the other two schedulers achieve over 20x speedup). This implies the non-adaptive scheduling can waste resources. GRADIENTCI and UCB are more robust. The average speedup of GRADIENTCI and UCB are 190x and 128x respectively. That shows the benefit of taking the speed of CI change into consideration during scheduling.

Note that the UCB method evaluated in this section is an enhanced algorithm of DAUB (Sabharwal, Samulowitz, and Tesauro 2016). Both UCB and DAUB use the same scheduling scheme, but UCB uses our novel CIestimator and CI-based pruning technique to ensure the ϵ -guarantee.